

Article

Phase-Transfer Catalyzed Microfluidic Glycosylation: A Small Change in Concentration Results in a Dramatic Increase in Stereoselectivity

Ilya V. Myachin ¹ and Leonid O. Kononov ^{1,*}

N.D. Zelinsky Institute of Organic Chemistry, Russian Academy of Sciences, Leninsky prosp. 47, 119991 Moscow, Russia

* Correspondence: kononov@ioc.ac.ru or leonid.kononov@gmail.com

Abstract: Phase-transfer catalysis (PTC) is widely used in glycochemistry for the preparation of aryl glycosides by the glycosylation reaction. While investigating the possibility of synthesis of 4-(3-chloropropoxy)phenyl sialoside (Neu5Ac-OCPP) from *N*-acetylsialyl chloride with *O*-acetyl groups (**1**), we have recently discovered a strong dependence of the PTC glycosylation outcome on the mixing mode: under batch conditions, only α -anomer of Neu5Ac-OCPP was obtained, albeit in low yield (13%), while under microfluidic conditions the yield of Neu5Ac-OCPP increased to 36%, although stereoselectivity decreased ($\alpha/\beta \leq 6.2$). Here, we report that the outcome of this reaction, performed under microfluidic conditions using a Comet X-01 micromixer (at 2 $\mu\text{L}/\text{min}$ flow rate), non-linearly depends on the concentration of *N*-acetylsialyl chloride **1** (5–200 mmol/L). The target Neu5Ac-OCPP was obtained in a noticeably higher yield (up to 66%) accompanied by enhanced stereoselectivity ($\alpha/\beta = 17:1\text{--}32:1$) in the high concentration range ($C > 50$ mmol/L), whereas the yield (10–36%) and especially, stereoselectivity ($\alpha/\beta = 0.9:1\text{--}6.2:1$) were lower in the low concentration range ($C \leq 50$ mmol/L). This dramatic stepwise increase in stereoselectivity above critical concentration (50 mmol/L) is apparently related to the changes in the presentation of molecules on the surface of supramers of glycosyl donor, which exist in different concentration ranges.

Keywords: phase-transfer catalysis; glycosylation; aryl glycosides; Janus aglycone; flow chemistry; microfluidics; Comet X-01 micromixer; supramers



Citation: Myachin, I.V.; Kononov, L.O. Phase-Transfer Catalyzed Microfluidic Glycosylation: A Small Change in Concentration Results in a Dramatic Increase in Stereoselectivity. *Catalysts* **2023**, *13*, 313. <https://doi.org/10.3390/catal13020313>

Academic Editor: Victorio Cadierno

Received: 22 November 2022

Revised: 25 January 2023

Accepted: 26 January 2023

Published: 1 February 2023



Copyright: © 2023 by the authors. Licensee MDPI, Basel, Switzerland. This article is an open access article distributed under the terms and conditions of the Creative Commons Attribution (CC BY) license (<https://creativecommons.org/licenses/by/4.0/>).

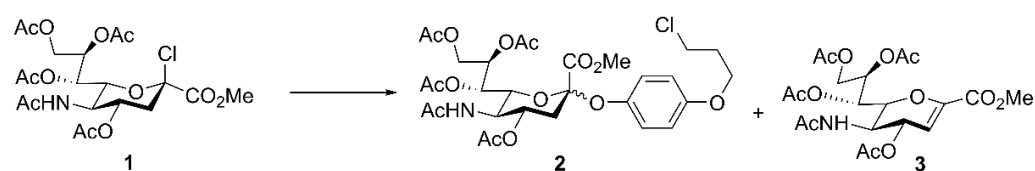
1. Introduction

Functionalized aryl glycosides have been widely used for the preparation of neoglycoconjugates [1–3], which are required in the rapidly developing fields of glycobiology [4,5] and glycomedicine [6–8]. We have recently introduced alkoxy-substituted aryl glycosides as promising Janus glycosides [9,10], the second generation of which contained 4-(3-chloropropoxy)phenyl (CPP) group [11–16] in aglycone.

Phase transfer catalysis (PTC) [17,18] is widely used for stereoselective synthesis [19,20] of various aryl glycosides [21,22] by the glycosylation reaction [23,24]. The method commonly utilizes a glycosyl halide [25] as a glycosyl donor (electrophile), a phenol as a glycosyl acceptor (nucleophile), AcOEt as a nonpolar phase and 10% aqueous Na_2CO_3 as a polar phase. The use of Bu_4NHSO_4 , which contains hydrophilic hydrogen sulphate anion with low nucleophilicity, as a phase transfer catalyst was shown [20,26] to be preferred over the use of halide ion-containing catalysts. Under these conditions, α -anomers of aryl sialosides have been reported to be exclusively formed from β -anomer of *N*-acetylsialyl chloride **1** along the $\text{S}_{\text{N}}2$ -like pathway [19,20,26–32].

While investigating the possibility of synthesis of CPP sialoside **2** from *N*-acetylsialyl chloride **1** by PTC glycosylation of 4-(3-chloropropoxy)phenol (CPP-OH) (Scheme 1), we recently discovered [33] a strong dependence of the outcome of PTC glycosylation of

CPP-OH (and other 4-alkoxyphenols) on the mixing mode. Under batch conditions, only α -anomer of **2** (a kinetically controlled product [23,24,34–36]) was obtained, albeit in low yield (13%), whereas under microfluidic conditions using a Comet X-01 micromixer, which has been widely used in glycosylation reactions [33,37–45], the yield of **2** increased to 36%, although stereoselectivity decreased ($\alpha/\beta \leq 6.2$). This unexpected loss of stereoselectivity under microfluidic conditions does not fit the current knowledge [20,46–48] on the origin of stereoselectivity of glycosylation with sialic acid derivatives (sialylation). However, the found phenomenon can be rationally discussed within the framework of supramer hypothesis (supramer approach) [49], according to which the real reacting species in many cases are supramolecular aggregates (supramers) rather than single molecules of reacting substances. According to the explanation suggested in [33], the efficiency of disaggregation/rearrangement of *N*-acetylsialyl chloride **1** supramers [49] varies under different mixing modes (in particular, at different flow rates). This makes the S_N1 -like pathway within the S_N1 – S_N2 -continuum of glycosylation mechanisms [34–36] possible under microfluidic conditions, leading to the formation of both anomers of CPP sialoside **2**. It was shown in our previous work [33] that the reaction under batch conditions requires 23 h to complete. The use of microfluidic conditions, which provide better mixing of reagents, allowed us to accelerate [50] the reaction and to decrease the reaction time to 3.7 h.



Scheme 1. Glycosylation reaction with *N*-acetylsialyl chloride **1** under flow conditions. Reagents and conditions: 4-(3-chloropropoxy)phenol (CPP-OH, 2 equiv.), Bu_4NHSO_4 (1 equiv.), AcOEt, 10% aq Na_2CO_3 , Comet X-01 micromixer (see Figure 1 for experimental setup). Flow rate 2 $\mu\text{L}/\text{min}$ was used. Concentration of **1** varied in 5–200 mmol/L range. See Table 1.

Table 1. Results of PTC glycosylation of CPP-OH by *N*-acetylsialyl chloride **1** under flow conditions at various concentrations.

| Entry ¹ | C, mmol/L | Yield of 2 , % ² | α/β ² | Yield of 3 , % ^{2,3} | Conversion of 1 , % ² |
|--------------------|-----------|------------------------------------|-----------------------------|--------------------------------------|-----------------------------------------|
| 1 ⁴ | 5 | 15 | 0.9 | 5 | 75 |
| 2 ⁴ | 10 | 12 | 1.0 | 8 | 66 |
| 3 | 15 | 10 | 2.5 | 2 | 69 |
| 4 ⁵ | 25 | 21 | 2.3 | 4 | 57 |
| 5 ⁶ | 35 | 14 | 4.3 | n. d. ⁷ | 58 |
| 6 ⁸ | 50 | 36 | 6.2 | 12 | 100 |
| 7 | 60 | 29 | 17.0 | 5 | 66 |
| 8 | 75 | 47 | 31.6 | 11 | 100 |
| 9 | 100 | 43 | 20.7 | 9 | 79 |
| 10 | 200 | 66 | 17.6 | 12 | 100 |

¹ Glycosylation conditions: 1 equiv. **1**, 2 equiv. CPP-OH, 1 equiv. Bu_4NHSO_4 , AcOEt, 10% aq Na_2CO_3 , 20 °C, Comet X-01 micromixer, flow rate 2 $\mu\text{L}/\text{min}$ (see Scheme 1 and Figure 1). ² Yields are quoted in molar percentages. The yields of aryl sialoside **2** and glycal **3**, conversion of **1** and the ratio of anomers $2\alpha/2\beta$ (α/β) were determined by ¹H NMR (600 MHz, CDCl_3) analysis of the worked-up reaction mixtures using 1,4-dinitrobenzene (δ 8.41 ppm) as the internal standard; the integral intensities of signals of α -H-3eq (δ 2.70 ppm (2α)), β -H-3eq (δ 2.65 ppm (2β)), 2.78 ppm (**1**), and H-3 (δ 5.99 ppm (**3**)) of the Neu5Ac residue were used. See Figures 2 and 3. ³ The yield of glycal **3** was calculated considering its presence in the starting *N*-acetylsialyl chloride **1** as an impurity (6.7% (mass.)), see Section 4.1). ⁴ The reaction was performed at 24 °C. ⁵ The reaction was performed at 22 °C. ⁶ The reaction was performed at 19 °C. ⁷ No data. The amount of glycal **3** in the reaction mixture after work-up (5.7% (mass.)) was lower than that in the sample of starting *N*-acetylsialyl chloride **1** used for the reaction. ⁸ Data from a previous study [33].

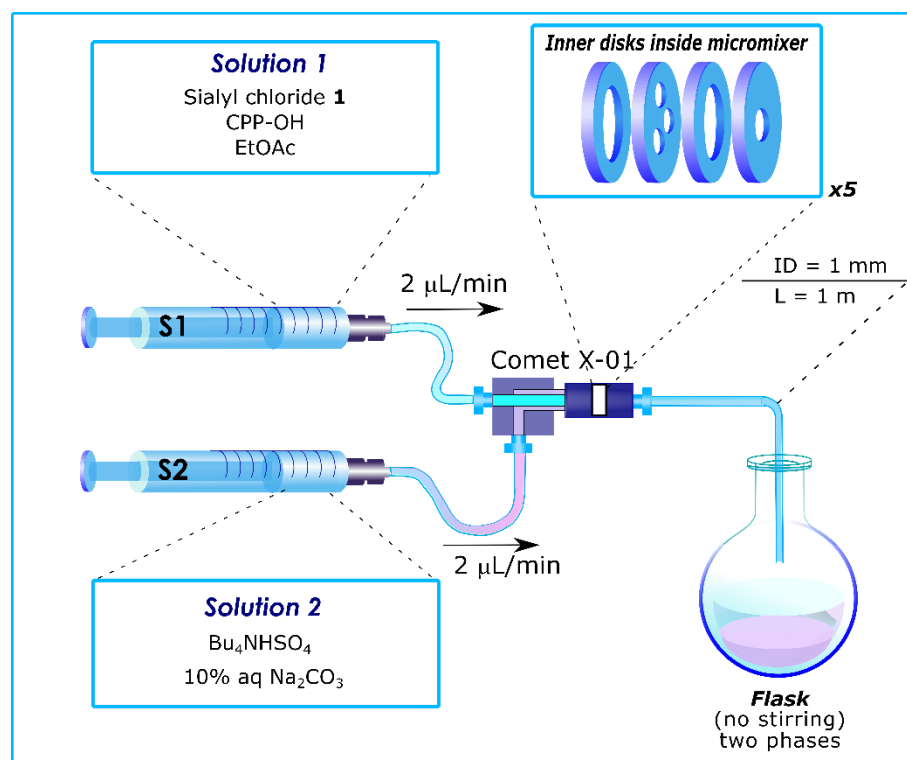


Figure 1. Flow reactor used for glycosylation experiments. S1, S2—syringes. Internal volume of Comet X-01 micromixer—0.1 mL, that of outlet capillary—0.785 mL. Adapted from [33] by permission.

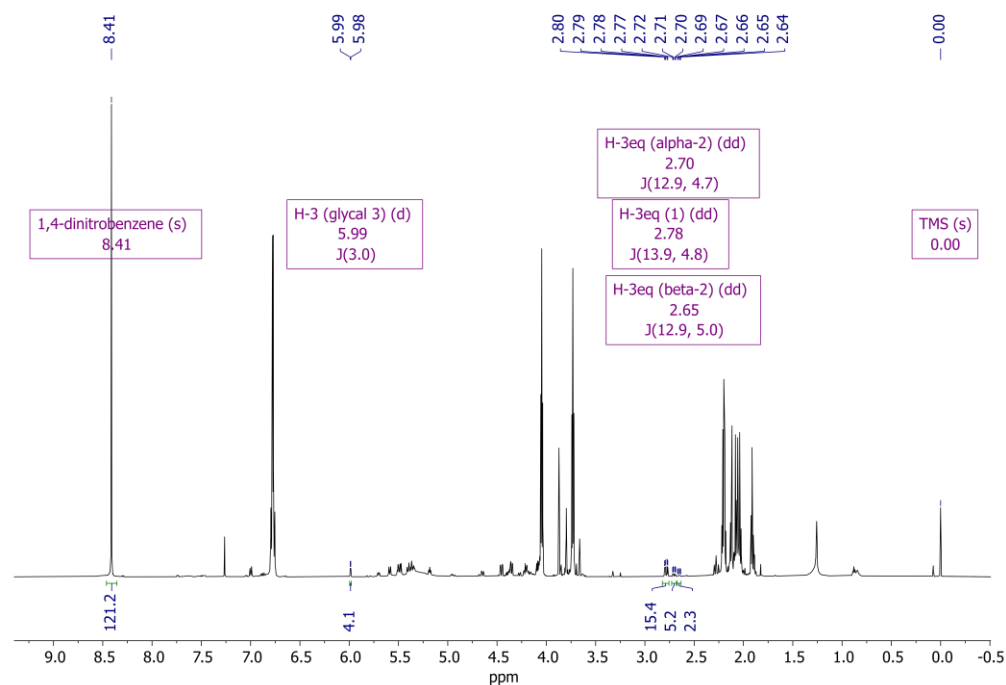


Figure 2. ^1H NMR spectrum (600.13 MHz, CDCl_3) of the worked-up reaction mixture (see Table 1, entry 4) illustrating determination of quantities of glycal 3 (5.99 ppm), *N*-acetylsialyl chloride 1 (2.78 ppm), α - and β -aryl sialosides 2 (2.70 and 2.65 ppm, respectively) relative to the standard—1,4-dinitrobenzene (8.41 ppm) by qNMR. Integral values correspond to the amounts (μmol) of the respective substances.

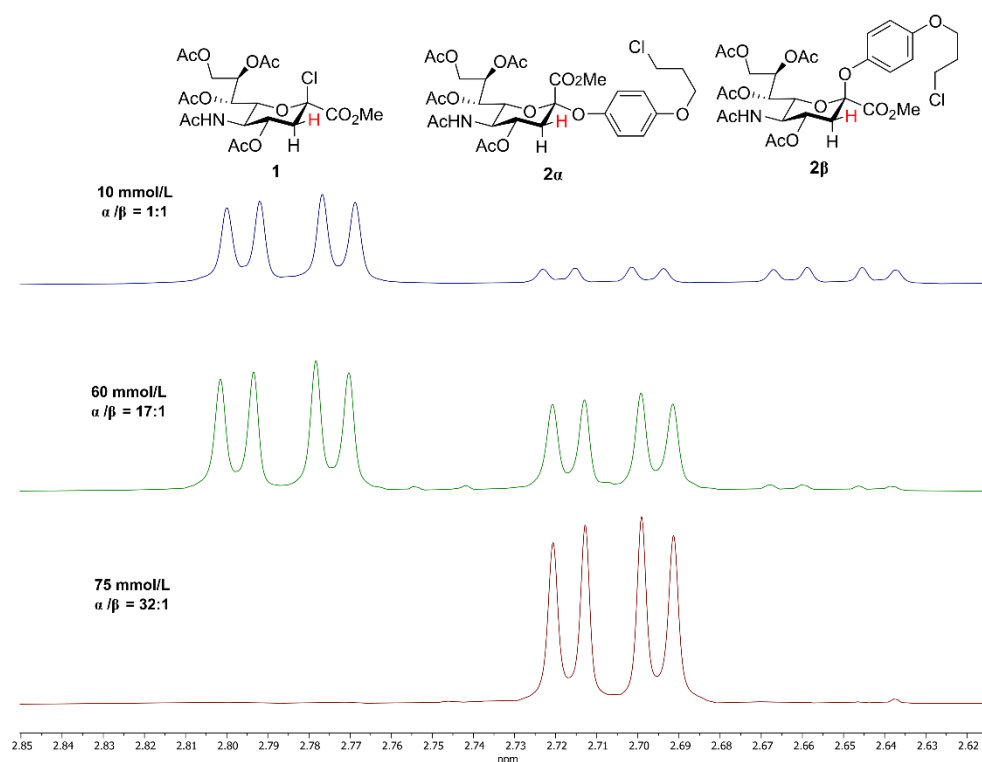


Figure 3. Part of the ^1H NMR spectra (600.13 MHz, CDCl_3) of the worked-up reaction mixtures showing H-3eq signals of *N*-acetylsialyl chloride **1** and α - and β -sialosides **2 α** and **2 β** : see entry 2 (blue line), entry 7 (green line) and entry 8 (red line) in Table 1.

The outcome of glycosylation (including stereoselectivity) is known to depend on the concentration of reactants (see Refs. [49,51–56]). In some cases, bimodal concentration dependence of reactivity/selectivity pattern has been observed which, according to supramer hypothesis (*vide supra*), can originate from changes in solution structure associated with rearrangements of supramers of reactants upon changes in concentration [49,51–58].

For this reason, we attempted to reveal how changes in concentration of *N*-acetylsialyl chloride **1** affect the outcome of the glycosylation reaction, shown in Scheme 1, under microfluidic conditions, and here we report the results obtained.

2. Results

Glycosylation reactions are typically performed at a 50 mmol/L concentration of glycosyl donor, which is de facto the “standard” concentration for glycosylation. It is this concentration that was used in our previous study [33], in which the influence of the mixing mode on the outcome of glycosylation was found (*vide supra*). In this study, we performed the glycosylation reaction, shown in Scheme 1, under microfluidic conditions using a Comet X-01 micromixer at various concentrations of *N*-acetylsialyl chloride **1** (5–200 mmol/L) while keeping the molar ratio of other reactants constant. Note that PTC reactions have earlier been performed under microfluidic conditions using a Comet X-01 micromixer [59] and other micromixers [60,61]. The flow rate was kept constant at 2 $\mu\text{L}/\text{min}$ since the highest yield and stereoselectivity had earlier been achieved [33] at this flow rate. The worked-up reaction mixtures were analyzed by ^1H qNMR using 1,4-dinitrobenzene as the internal standard to give the yield of aryl sialoside **2** and glycal **3**, conversion of **1** and the ratio of anomers (α/β) of CPP sialoside **2** (see Table 1, Figures 2–4).

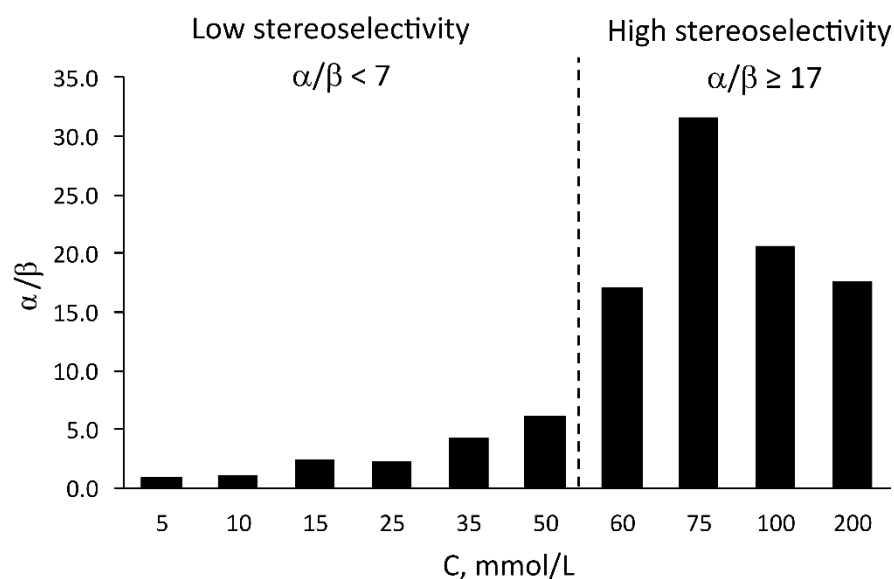


Figure 4. Dependence of stereoselectivity (α/β) of glycosylation on concentration (C) of *N*-acetylsialyl chloride **1** (see Scheme 1 and Table 1). Dashed line separates two concentration ranges: at $C \leq 50$ mmol/L, stereoselectivity is low ($\alpha/\beta < 7$), while at $C > 50$ mmol/L, stereoselectivity is high ($\alpha/\beta \geq 17$).

Analysis of the results obtained (Table 1, Figure 4) immediately revealed the existence of two distinct concentration ranges, separated by a “critical” [58,62] concentration (50 mmol/L), with remarkably different outcome of glycosylation (Scheme 1), which non-linearly depends on concentration of *N*-acetylsialyl chloride **1**.

In the low concentration range ($C \leq 50$ mmol/L), stereoselectivity gradually increases with increase in concentration: the reaction is completely unselective at 5–10 mmol/L ($\alpha/\beta = 0.9:1-1:1$, entries 1 and 2 in Table 1), moderately selective at 15–25 mmol/L ($\alpha/\beta = 2.3:1-2.5:1$, entries 3 and 4 in Table 1) and fairly stereoselective at 35–50 mmol/L ($\alpha/\beta = 4.3:1-6.2:1$, entries 5 and 6 in Table 1). In the high concentration range ($C > 50$ mmol/L), the stereoselectivity of the reaction is remarkably high ($\alpha/\beta \geq 17:1$) and reaches maximum at 75 mmol/L ($\alpha/\beta = 31.6:1$, entry 8 in Table 1).

The yield of CPP sialoside **2** generally follows a similar trend, being higher in the high concentration range ($C > 50$ mmol/L) and reaching 66% at 200 mmol/L as compared with the yield (10–36%) in the low concentration range ($C \leq 50$ mmol/L). Conversion of **1** tends to be lower in the low concentration range ($C < 50$ mmol/L, average 65%) than in the high concentration range ($C \geq 50$ mmol/L, average 89%).

Similarly to other sialylation reactions [20,46–48], glycal **3** was formed as a by-product in 2–12% yield in reactions performed at all concentrations studied with one exception. The amount of glycal **3** in the reaction mixture obtained at 35 mmol/L (entry 5 in Table 1) after work-up (5.7% (mass.)) was lower than that in the starting *N*-acetylsialyl chloride **1** (6.7% (mass.)), probably due to side processes which consumed glycal **3**. According to our experience [63,64], glycosylation reactions involving *N*-acetylsialyl chloride **1** are sometimes accompanied by consumption of glycal **3**, which is present (in variable amounts, its content $\leq 15\%$) in all preparations of *N*-acetylsialyl chloride **1** as an impurity (unpublished results). Note that since *N*-acetylsialyl chloride **1** decomposes on silica gel and does not crystallize, purification of it by chromatography on silica gel or crystallization is not feasible.

3. Discussion

3.1. Flow in Microfluidic System and the Choice of Flow Rate

The Reynolds number [65] of a typical microfluidic system is low (≤ 1000) [66–68]. A low Reynolds number suggests a laminar flow, even in reactors in which a biphasic PTC reaction proceeds [60], and “ensures that there is no turbulence and hence no back-mixing within the reactor” [67]. A complicated structure of the Comet X-01 micromixer (Figure 1),

where flow is split into three and merged back into one (repeated five times), remotely resembles a “split-and-recombine” microreactor [69–71] featured by “chaotic mixing” [70,72], which ensures efficient mixing regardless of the Reynolds number [72]. Although numerical modeling of flow was performed not only for the simplest T-mixers [73–75] and Y-mixers [75], but also for a more sophisticated “showerhead micromixer” [76] and “split-and-recombine” microreactor [69,70], we could not find the corresponding information regarding the Comet X-01 micromixer.

There are situations in which an increase in the flow rate (hence, the Reynolds number) leads to a decrease in reaction time [45]. However, increasing the flow rate is not a panacea: if the flow rate is too high, then the reactants simply will not have enough time to react inside the reactor.

In a previous study [33], we varied the flow rate from 2 to 1000 $\mu\text{L}/\text{min}$ and noticed a tendency for the yield to decrease (from 36% to 11%) with an increase in the flow rate from 2 to 250 $\mu\text{L}/\text{min}$. This leads us to believe that a 2 $\mu\text{L}/\text{min}$ low flow rate is preferable for the reaction in question.

The residence time for all experiments performed in this work (Table 1) is the same—3.7 h, which corresponds to a 2 $\mu\text{L}/\text{min}$ flow rate. After this time, the reaction is complete (100% conversion) at 50 mmol/L concentration of *N*-acetylsialyl chloride **1** (see entry 6 in Table 1) [33]. Reactions at other concentrations were stopped after this time, and conversions were determined by qNMR as described in Section 4.3. The differences in conversions found suggest differences in reactivity of *N*-acetylsialyl chloride **1** at different concentrations.

3.2. Concentration-Dependent Stereoselectivity of the Sialylation

The discovery of bimodal concentration dependence of the yield of CPP sialoside **2** and especially of stereoselectivity of glycosylation (see Section 2) is remarkable. Noteworthy, similar bimodal behavior has already been described for other glycosylation reactions in our previous publications [51–56], suggesting generality of the phenomenon (see also Section 3.4). The most striking finding is that a *small change* in concentration (from 50 to 60 mmol/L) results in an almost *tree-fold increase* in stereoselectivity from $\alpha/\beta = 6.2:1$ (entry 6 in Table 1) to $\alpha/\beta = 17:1$ (entry 7 in Table 1). This observation suggests that when performing glycosylation, one should be aware of a possibly strong influence of concentration on the reaction outcome and should preferably perform the reaction at a variety of concentrations seeking the concentration range where the required yield and stereoselectivity can be achieved. This screening of concentrations can be performed “randomly” by a traditional “trial-and-error” approach. For the rational selection of concentrations for glycosylation, we, however, recommend using the so-called “supramer analysis” [52,55–58] of solutions whenever possible. The supramer analysis, which is an integral part of the supramer approach being developed by us (vide supra, for detailed discussion of the approach, see a review [49]), allows one to distinguish solutions (with different concentrations) that are featured by different solution structures. Essentially, the supramer analysis is based on an analysis of the plots of numerical data related to the reaction solution (such as the specific optical rotation [51–53,55,56,58,62,77–79], scattered light intensity [52,53,56–58,62,79,80] or intensity of bands in IR spectra [51,53]) against concentration for the presence of discontinuities, which are taken as critical [58,62] concentrations that separate concentration ranges, where supramers with different structures and hence chemical properties of the solute exist. In other words, the rational selection of concentrations for performing glycosylation reactions takes into consideration changes in solution structure with concentration.

In the particular case of PTC glycosylation, application of supramer analysis is problematic for technical reasons associated with the biphasic nature of the reaction mixture. Nevertheless, it is worthy of note that the existence of supramers, which incorporate molecules of *N*-acetylsialyl chloride **1**, in the reaction solution (Scheme 1) has earlier been corroborated by dynamic light scattering study of solutions of *N*-acetylsialyl chloride **1** both in anhydrous AcOEt and in AcOEt saturated with water [80].

3.3. Supramer Approach for the Explanation of the Phenomenon of Bimodality of Glycosylation

Recent studies revealed [81–89] that even macroscopically homogeneous aqueous and non-aqueous solutions of low-molecular-mass non-amphiphilic compounds can contain nano- and mesoscale heterogeneities (size from ca. 1 nm to 10^2 – 10^3 nm) that are kinetically stable, although very small interaction energy, which does not exceed $k_B T$ [90], is involved. The most probable reason for their existence and omnipresence is the “solvophobicity-driven mesoscale” structuring [88] promoted by even minute amounts of “solvophobic admixtures” [49,88] that are present in most “research-grade compounds of p.a. purity and even after special in-lab purification procedures” [85], since “no truly pure chemicals exist” [88].

Considering the presence of such heterogeneities, supramers in our terminology [49], which belong to the realm of soft matter, we have been developing the supramer approach (vide supra) for the description of chemical reactions (see Refs. [49,57,58,79]). According to the supramer approach, the presentation (spatial orientation) of molecules on the surface of supramers of a glycosyl donor may play an important role in determining reaction stereoselectivity.

In our previous article [33], we proposed that, under microfluidic conditions, the product with retained anomeric configuration (2β) can only be formed along the S_N1 -like pathway while the major product with inverted anomeric configuration (2α) is mainly formed along the S_N2 -like pathway (as commonly stated based on the results of PTC glycosylations under batch conditions).

Here, we go further and hypothesize that the glycosylation reaction (Scheme 1) performed both under batch and microfluidic conditions follows *only* the S_N1 -like pathway (for an alternative opinion, see [35,36]). In such a case, we need to suppose that concentration-induced changes in stereoselectivity, and especially the dramatic stepwise increase in stereoselectivity above critical concentration (50 mmol/L), found in this study, are related to the changes in the presentation of molecules on the surface of supramers of *N*-acetylsialyl chloride **1**, which exist in different concentration ranges.

Three types of supramers featured by different presentation of molecules of *N*-acetylsialyl chloride **1** on the surface can be envisioned (Figure 5):

- Type I supramers: both sides of a glycosyl cation formed from *N*-acetylsialyl chloride **1** along the S_N1 -like pathway are accessible for the attack of nucleophile leading to unselective reaction (see Figure 5a).
- Type II supramers: only one side of a glycosyl cation formed from *N*-acetylsialyl chloride **1** along the S_N1 -like pathway is accessible for the attack of a nucleophile leading to formation of α -anomer of glycoside **2** only (see Figure 5b).
- Type III supramers: only one side of a glycosyl cation formed from *N*-acetylsialyl chloride **1** along the S_N1 -like pathway is accessible for the attack of a nucleophile leading to formation of β -anomer of glycoside **2** only (see Figure 5c).

Thus, the following scenario can be anticipated. At the two lowest concentrations (5–10 mmol/L) belonging to the low concentration range, type I supramers (and/or equal amounts of type II and type III supramers) are apparently formed, and the glycosylation reaction is unselective ($\alpha/\beta = 0.9:1$ – $1:1$, entries 1 and 2 in Table 1). At somewhat higher concentrations (15–25 mmol/L) belonging to the low concentration range, although type I supramers still dominate, type II supramers begin to form, and the glycosylation reaction is moderately selective ($\alpha/\beta = 2.3:1$ – $2.5:1$, entries 3 and 4 in Table 1). At even higher concentrations (35–50 mmol/L) belonging to the low concentration range, although type I supramers (and/or type III supramers) are still present, type II supramers begin to dominate, and the glycosylation reaction is fairly selective ($\alpha/\beta = 4.3:1$ – $6.2:1$, entries 5 and 6 in Table 1). In the high concentration range ($C = 60$ – 200 mmol/L), type II supramers are mainly formed, although type I supramers (and/or type III supramers) are still present, and the glycosylation reaction is highly stereoselective ($\alpha/\beta = 17.0:1$ – $31.6:1$, entries 7–10 in Table 1). Note that while the presence of type III supramers cannot be excluded at all

concentrations studied, their presence is *required* at the lowest concentration (5 mmol/L) where the glycosylation reaction is slightly β -selective (entry 1 in Table 1).

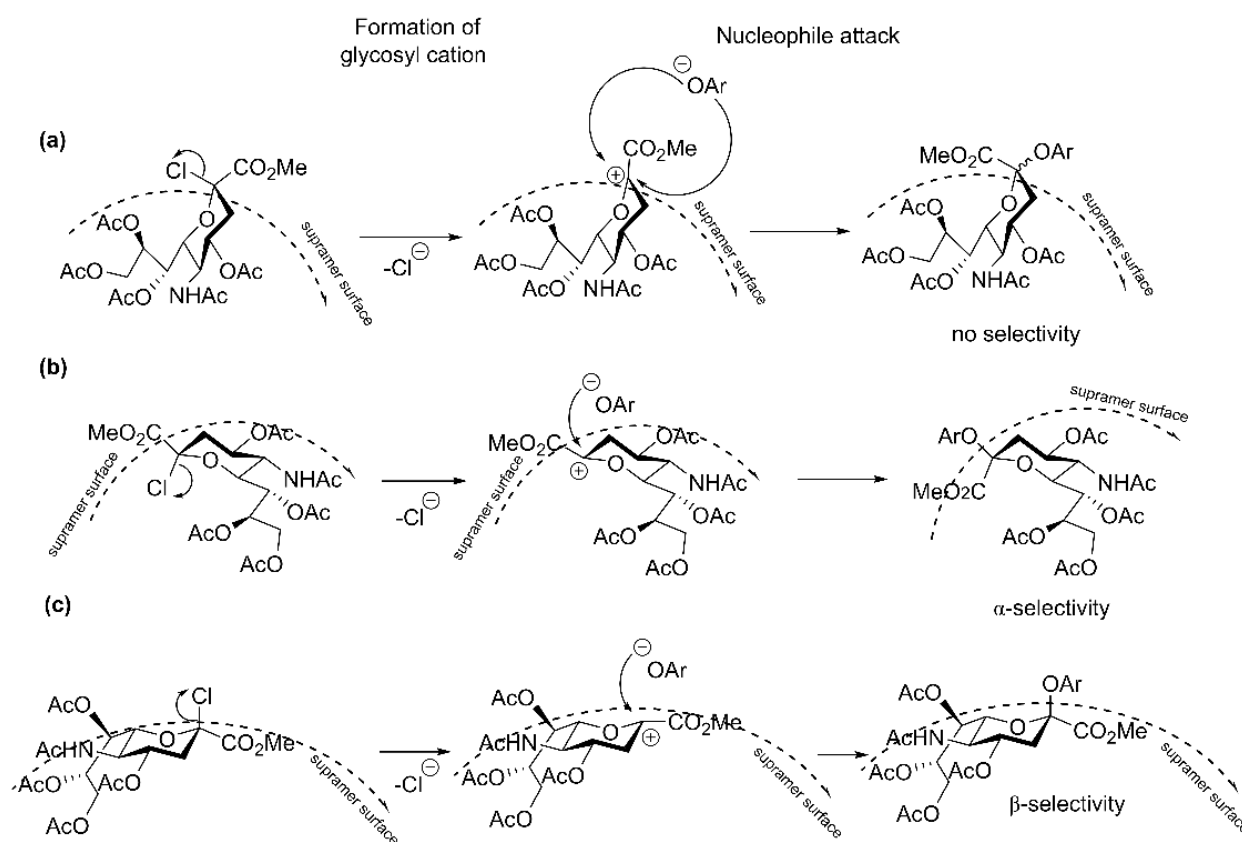


Figure 5. Possible presentations of *N*-acetylsialyl chloride **1** molecule on the surface of a supramer (dashed line): (a) Type I supramers; both sides of a glycosyl cation formed from *N*-acetylsialyl chloride **1** are accessible for the attack of a nucleophile leading to unselective reaction. (b) Type II supramers and (c) type III supramers; only one side of a glycosyl cation formed from *N*-acetylsialyl chloride **1** is accessible for a nucleophile attack leading to formation of one anomer only (α or β , respectively).

Such changes on the surface of supramers remind of metal nanoparticles, the shape of which can affect their chemical properties [91,92]. Although it is quite possible that the surface of supramers may likewise be described as having a “shape”, other studies considered mesoscale structures (related to supramers) in solutions as aggregates without well-defined shape [93–95]. At the current level of knowledge, there are no physical methods capable of determining the shape of supramers. Note that multiangle light scattering can determine the shape of only monodisperse scattering objects for which fitting to Lorenz–Mie model can be performed [88].

Another analogy can be drawn with crystal growth. It is widely known that crystals grow into certain shapes. It happens that a crystal grows much faster in certain directions than in others, which determines its spatial geometry: cube, needle, etc. However, at the beginning of crystal growth, when there is no observable solid phase yet, a group of molecules is organized in such a way (in a supramer of such a shape) to determine a certain spatial geometry. This supramer attaches molecules to itself much more easily at the one side, and much more difficultly at the other one. Apparently, this is a common feature since spherical crystals (growing uniformly in all directions) do not exist. Note that formation of supramers (pre-nucleation clusters) with different structure has been reported [96] in undersaturated solutions of fenoxycarb in isopropyl alcohol.

As was mentioned above, average conversion of *N*-acetylsialyl chloride **1** in the low concentration range ($C < 50$ mmol/L) is noticeably lower (65%) than that (89%) in the high

concentration range ($C \geq 50$ mmol/L). This may indicate that with increasing concentration, supramers become looser, allowing molecules of nucleophile (CPP-OH) to reach the core of supramers and react with *all* molecules of *N*-acetylsialyl chloride **1**. Note that formation of tight supramers of a glycosyl donor, featured by lowered reactivity, apparently due to poor accessibility of the molecules located in the core of supramers in dilute solutions, was detected for another reaction [56], suggesting a possibility of this scenario in our case too. The currently accepted mechanism of glycosylation reaction [34,35] does not allow rational discussion of effect of concentration (see Ref. [36] for the discussion of the importance of concentration in glycosylation reaction) on the completeness and stereoselectivity of glycosylation.

3.4. Bimodality of Glycosylation in Glycochemistry

The observed bimodal concentration dependence of yield and stereoselectivity of PTC glycosylation (see Sections 2 and 3.2) is not a unique phenomenon. We have previously reported several examples of bimodal behavior in glycosylation reactions involving diverse glycosyl donors such as sialic acid thioglycosides [51–53,56], arabinofuranose thioglycoside [55] and arabinofuranose glycosyl bromide [54,58]. In all cases studied, concentration ranges separated by critical concentrations were revealed by supramer analysis (see Section 3.2) using polarimetry [51,52,55,56,58,62,77–79], light scattering [52,56–58,62,79,80] or IR spectroscopy [51]. At concentrations exceeding a critical concentration, the product yield was higher and virtually did not depend on concentration [51–53,55,56], suggesting formation of reacting species (supramers) of glycosyl donor with similar structures, hence reactivities, but considerably different from those formed in more dilute solutions. In one case, at concentrations below the critical concentration, stereoselectivity of glycosylation experienced a dramatic rise (unlike results reported here) as compared to that in more concentrated solutions [54,58]. In other cases, stereoselectivity at a critical concentration corresponded to a maximum [52,55] or a minimum [52].

In our opinion, the generality of phenomenon of bimodality of glycosylation outcome strongly suggests the importance of considering changes in solution structure associated with rearrangements of supramers of reactants upon changes in concentration. We speculate that similar dramatic changes in the reaction solution structure, hence the reaction outcome, can occur upon changes of the reaction solvent [97,98] or the length of the hydrocarbon chain in a reactant [12].

4. Materials and Methods

4.1. General Methods

The reactions were performed with the use of commercial reagents (Aldrich, Saint Louis, MO, USA; Fluka, Seelze, Germany; Acros Organics, Geel, Belgium). *N*-Acetylsialyl chloride **1** [64] and 4-(3-chloropropoxy)phenol (CPP-OH) [99] were synthesized according to previously reported procedures. *N*-Acetylsialyl chloride **1** contained 90.5% (mass.) of the chloride **1** and 6.7% (mass.) of glycal **3** [64,100] as an impurity (^1H qNMR data using 1,4-dinitrobenzene (δ_{H} 8.41 ppm) as the internal standard). Solvents were purified and dried (where appropriate) according to standard procedures [101]. Ethyl acetate was purified by distillation over P_2O_5 and kept over molecular sieves (MS) 4 Å under argon before use. NMR spectra were recorded on a Bruker AVANCE 600 spectrometer (600.13 MHz for ^1H , Billerica, MA, USA). The ^1H NMR chemical shifts are given relative to the signal of internal Me_4Si (δ_{H} 0.0 ppm).

4.2. Flow Reactor

The design of the flow reactor (Figure 1) was identical to that used in a previous study [33]. In brief, the reaction in flow was performed with the use of a syringe pump (AL-1200, World Precision Instruments, Sarasota, FL, USA, www.wpiinc.com (accessed on 20 January 2023)), a Comet X-01 micromixer (PTFE, Techno Applications Co., Ltd., Tokyo, Japan) and two identical syringes **S1** and **S2** (5 or 10 mL each, cylinder–polypropylene,

piston—polyethylene, Becton, Dickinson & Co., Franklin Lakes, NJ, USA, www.bd.com (accessed on 20 January 2023)). The internal diameter of all capillaries (PTFE) was 1.0 mm; the length of the capillaries between syringe **S1** and the micromixer and between syringe **S2** and the micromixer was 0.5 m each, and the length of the output capillary (which served as a microtube reactor) was 1.0 m. Internal volume of Comet X-01 micromixer—0.1 mL, that of outlet capillary—0.785 mL.

4.3. General Glycosylation Procedure

Glycosylation was performed in flow mode under PTC conditions at ambient temperature (19–24 °C, see Table 1 for specific values) using the flow reactor (see Section 4.2 and Figure 1), essentially as described in a previous study [33].

N-acetylsialyl chloride **1** (20–80 mg, 1 equiv.) and CPP-OH (2 equiv.) were dissolved in anhydrous AcOEt (0.8–8.0 mL) under argon to give the required concentration of *N*-acetylsialyl chloride **1** (5–200 mmol/L, see Table 1). This solution and an additional volume of argon gas (1.5 mL) were collected in the first syringe **S1** (see Figure 1). The second syringe **S2** was filled with a solution of Bu₄NHSO₄ (1 equiv.) in 10% aq Na₂CO₃ (volume of the solution in syringe **S2** was equal to the volume of AcOEt in syringe **S1**) and air (1.5 mL). Both solutions were pumped through a Comet X-01 micromixer at flow rate 2 μL/min for each syringe using a syringe pump; the resulting mixture was allowed to flow through a microtube reactor (internal diameter: 1 mm, length 1.0 m) with total residence time 3.7 h, and then collected in a receiving flask without stirring (see Figure 1). After the end of the process, the collected mixture was diluted with 10% aq Na₂CO₃ (10 mL) and extracted by AcOEt (5 × 15 mL). The combined organic extracts were filtered through a mixture of Celite and anhydrous Na₂SO₄ (1:1, *v/v*) and dried in vacuo to give a yellow syrup, which was analyzed by ¹H qNMR (600 MHz, CDCl₃) using 1,4-dinitrobenzene (δ_H 8.41 ppm) as the internal standard (Figure 2) to give the yields of aryl sialoside **2** and glycal **3**, conversion of **1** and the ratio of anomers (α/β, Figures 3 and 4) of CPP sialoside **2** (see Table 1). TLC mobilities (*R_f* values) and ¹H NMR data (Figures 2 and 3) for all compounds correspond to those published (for more details see Ref. [33]).

5. Conclusions

The preparation of aryl sialosides using phase-transfer catalyzed glycosylation is a well-known highly stereoselective method [19,20]. In this study, we have shown that in fact, stereoselectivity of this reaction, performed under microfluidic conditions, non-linearly depends on concentration of glycosyl donor in addition to the previously found [33] dependence of stereoselectivity on the mixing mode and flow rate. Thus, it was found that by changing only the concentration, it is possible to switch the reaction from non-selective (α/β = 1:1, 5 mmol/L) to almost stereospecific (α/β = 32:1, 75 mmol/L). Explaining this phenomenon, we came to the conclusion that the true reacting species in the reaction solution are supramers [49] rather than the parent molecules. The use of a flow reactor allows one to easily scale up the production of CPP sialoside **2** in a relatively high yield and high stereoselectivity.

Author Contributions: Conceptualization, I.V.M. and L.O.K.; methodology, I.V.M. and L.O.K.; investigation, I.V.M.; writing—original draft preparation, I.V.M.; writing—review and editing, L.O.K.; visualization, I.V.M. and L.O.K.; supervision, L.O.K.; project administration, L.O.K. All authors have read and agreed to the published version of the manuscript.

Funding: This research received no external funding.

Data Availability Statement: Not applicable.

Conflicts of Interest: The authors declare no conflict of interest.

References

1. Magnusson, G.; Chernyak, A.Y.; Kihlberg, J.; Kononov, L.O. Synthesis of Neoglycoconjugates. In *Neoglycoconjugates: Preparation and Application*; Lee, Y.C., Lee, R.T., Eds.; Academic Press Inc.: San Diego, CA, USA, 1994; pp. 53–143.
2. Larsen, K.; Thygesen, M.B.; Guillaumie, F.; Willats, W.G.T.; Jensen, K.J. Solid-phase Chemical Tools for Glycobiology. *Carbohydr. Res.* **2006**, *341*, 1209–1234. [[CrossRef](#)]
3. Villadsen, K.; Martos-Maldonado, M.C.; Jensen, K.J.; Thygesen, M.B. Chemoselective Reactions for the Synthesis of Glycoconjugates from Unprotected Carbohydrates. *ChemBioChem* **2017**, *18*, 574–612. [[CrossRef](#)]
4. Seeberger, P.H. Chemical Glycobiology: Why Now? *Nat. Chem. Biol.* **2009**, *5*, 368–372. [[CrossRef](#)]
5. Solís, D.; Bovin, N.V.; Davis, A.P.; Jiménez-Barbero, J.; Romero, A.; Roy, R.; Smetana, K., Jr.; Gabius, H.-J. A Guide into Glycosciences: How Chemistry, Biochemistry and Biology Cooperate to Crack the Sugar Code. *Biochim. Biophys. Acta Gen. Subj.* **2015**, *1850*, 186–235. [[CrossRef](#)]
6. Stallforth, P.; Lepenies, B.; Adibekian, A.; Seeberger, P.H. Carbohydrates: A Frontier in Medicinal Chemistry. *J. Med. Chem.* **2009**, *52*, 5561–5577. [[CrossRef](#)]
7. Bhatia, S.; Dimde, M.; Haag, R. Multivalent Glycoconjugates as Vaccines and Potential Drug Candidates. *Med. Chem. Commun.* **2014**, *5*, 862–878. [[CrossRef](#)]
8. Rademacher, C.; Seeberger, P.H. (Eds.) *Carbohydrates as Drugs*, 1st ed.; Springer International Publishing: Cham, Switzerland, 2014. [[CrossRef](#)]
9. Abronina, P.I.; Zinin, A.I.; Romashin, D.A.; Tereshina, V.V.; Chizhov, A.O.; Kononov, L.O. Application of a Janus Aglycon with Dual Function in Benzyl-Free Synthesis of Spacer-Armed Oligosaccharide Fragments of Polysaccharides from *Rhizobacterium Azospirillum brasilense* sp7. *Carbohydr. Res.* **2018**, *464*, 28–43. [[CrossRef](#)]
10. Abronina, P.I.; Shvyrkina, J.S.; Zinin, A.I.; Chizhov, A.O.; Kononov, L.O. Synthesis of Selectively Protected α -(1-3)-, α -(1-5)-Linked Octasaccharide Fragment, Containing Janus Aglycon, Related to Branching Region of Mycobacterial Polysaccharides. *Russ. Chem. Bull.* **2022**, *71*, 2740–2750.
11. Abronina, P.I.; Zinin, A.I.; Malysheva, N.N.; Stepanova, E.V.; Chizhov, A.O.; Torgov, V.I.; Kononov, L.O. A Novel Glycosyl Donor with a Triisopropylsilyl Nonparticipating Group in Benzyl-Free Stereoselective 1,2-*cis*-Galactosylation. *Synlett* **2017**, *28*, 1608–1613. [[CrossRef](#)]
12. Stepanova, E.V.; Podvalnyy, N.M.; Abronina, P.I.; Kononov, L.O. Length Matters: One Additional Methylene Group in a Reactant is Able to Affect the Reactivity Pattern and Significantly Increase the Product Yield. *Synlett* **2018**, *29*, 2043–2045. [[CrossRef](#)]
13. Stepanova, E.V.; Abronina, P.I.; Zinin, A.I.; Chizhov, A.O.; Kononov, L.O. Janus Glycosides of Next Generation: Synthesis of 4-(3-Chloropropoxy)Phenyl and 4-(3-Azidopropoxy)Phenyl Glycosides. *Carbohydr. Res.* **2019**, *471*, 95–104. [[CrossRef](#)] [[PubMed](#)]
14. Stepanova, E.V.; Zinin, A.I.; Abronina, P.I.; Chizhov, A.O.; Kononov, L.O. Azidation of Partially Protected Carbohydrate Derivatives: Efficient Suppression of Acyl Migration. *Synlett* **2020**, *31*, 1491–1496. [[CrossRef](#)]
15. Abronina, P.I.; Malysheva, N.N.; Zinin, A.I.; Karpenko, M.Y.; Kolotyrkina, N.G.; Kononov, L.O. Trifluoroacetic Acid-Promoted Ring Contraction in 2,3-Di-*O*-silylated *O*-Galactopyranosides and Hemiacetals. *Synlett* **2022**, *33*, 473–477. [[CrossRef](#)]
16. Abronina, P.I.; Malysheva, N.N.; Stepanova, E.V.; Shvyrkina, J.S.; Zinin, A.I.; Kononov, L.O. Five Triisopropylsilyl Substituents in Ara- β -(1 \rightarrow 2)-Ara Disaccharide Glycosyl Donor Make Unselective Glycosylation Reaction Stereoselective. *Eur. J. Org. Chem.* **2022**, *2022*, e202201110. [[CrossRef](#)]
17. Dehmlow, E.V.; Dehmlow, S.S. *Phase Transfer Catalysis*, 3rd ed.; Wiley VCH: Weinheim, Germany, 1993; p. 499.
18. Otevreil, J.; Waser, M. Asymmetric Phase-Transfer Catalysis—From Classical Applications to New Concepts. In *Asymmetric Organocatalysis: New Strategies, Catalysts, and Opportunities*; Albrecht, L., Albrecht, A., Dell'Amico, L., Eds.; WILEY-VCH GmbH: Weinheim, Germany, 2023; Volume 2, pp. 71–120. [[CrossRef](#)]
19. Roy, R. Phase Transfer Catalysis in Carbohydrate Chemistry. In *Handbook of Phase Transfer Catalysis*; Sasson, Y., Neumann, R., Eds.; Springer: Dordrecht, The Netherlands, 1997; pp. 244–275. [[CrossRef](#)]
20. Roy, R.; Tropper, F.D.; Cao, S.; Kim, J.M. Anomeric Group Transformations Under Phase-Transfer Catalysis. In *Phase-Transfer Catalysis*; Halpern, M., Ed.; ACS Symposium Series; American Chemical Society: Washington, DC, USA, 1997; Volume 659, pp. 163–180. [[CrossRef](#)]
21. Yang, Y.; Yu, B. Recent Advances in the Chemical Synthesis of C-Glycosides. *Chem. Rev.* **2017**, *117*, 12281–12356. [[CrossRef](#)]
22. Dimakos, V.; Taylor, M.S. Recent Advances in the Direct *O*-Arylation of Carbohydrates. *Org. Biomol. Chem.* **2021**, *19*, 514–524. [[CrossRef](#)]
23. Demchenko, A.V. *Handbook of Chemical Glycosylation: Advances in Stereoselectivity and Therapeutic Relevance*; Wiley-VCH: Weinheim, Germany, 2008. [[CrossRef](#)]
24. Ágoston, K.; Watt, G.M. 2.04—Methods for *O*-Glycoside Synthesis. In *Comprehensive Glycoscience*, 2nd ed.; Barchi, J.J., Vidal, S., Eds.; Elsevier: Oxford, UK, 2021; Volume 2, pp. 103–159. [[CrossRef](#)]
25. Singh, Y.; Geringer, S.A.; Demchenko, A.V. Synthesis and Glycosidation of Anomeric Halides: Evolution from Early Studies to Modern Methods of the 21st Century. *Chem. Rev.* **2022**, *122*, 11701–11758. [[CrossRef](#)]
26. Roy, R.; Tropper, F.D.; Romanowska, A.; Letellier, M.; Cousineau, L.; Meunier, S.J.; Boratynski, J. Expedient Syntheses of Neoglycoproteins Using Phase-Transfer Catalysis and Reductive Amination as Key Reactions. *Glycoconj. J.* **1991**, *8*, 75–81. [[CrossRef](#)]

27. Rothermel, J.; Faillard, H. Phase-transfer-catalyzed Synthesis of Aryl α -Ketosides of *N*-Acetylneuraminic Acid. A 2-Methylfluoran-6-yl Glycoside of *N*-Acetylneuraminic Acid, 2-Methyl-6-(5-acetamido-3,5-dideoxy- α -D-glycero-D-galacto-nonulopyranosylonic acid)xanthen-9-spiro-1'-isobenzofuran-3'-one, a New Substrate for Neuraminidase Assay. *Carbohydr. Res.* **1990**, *196*, 29–40. [[CrossRef](#)]
28. Roy, R.; Tropper, F. Stereospecific Synthesis of Aryl β -D-*N*-Acetylglucopyranosides by Phase Transfer Catalysis. *Synth. Commun.* **1990**, *20*, 2097–2102. [[CrossRef](#)]
29. Roy, R.; Andersson, F.O.; Harms, G.; Kelm, S.; Schauer, R. Synthesis of Esterase-Resistant 9-*O*-Acetylated Polysialoside as Inhibitor of Influenza C Virus Hemagglutinin. *Angew. Chem. Int. Ed. Engl.* **1992**, *31*, 1478–1481. [[CrossRef](#)]
30. Gan, Z.H.; Roy, R. Facile Preparation of Divalent Sialoside Derivatives by Olefin Metathesis Reaction. *Tetrahedron* **2000**, *56*, 1423–1428. [[CrossRef](#)]
31. Gan, Z.; Roy, R. Sialoside Clusters as Potential Ligands for Siglecs (Sialoadhesins). *Can. J. Chem.* **2002**, *80*, 908–916. [[CrossRef](#)]
32. Carlescu, I.; Osborn, H.M.I.; Desbrieres, J.; Scutaru, D.; Popa, M. Synthesis of Poly(aspartimide)-Based Bio-Glycoconjugates. *Carbohydr. Res.* **2010**, *345*, 33–40. [[CrossRef](#)]
33. Myachin, I.V.; Mamirgova, Z.Z.; Stepanova, E.V.; Zinin, A.I.; Chizhov, A.O.; Kononov, L.O. Black Swan in Phase Transfer Catalysis: Influence of Mixing Mode on the Stereoselectivity of Glycosylation. *Eur. J. Org. Chem.* **2022**, *2022*, e202101377. [[CrossRef](#)]
34. Adero, P.O.; Amarasekara, H.; Wen, P.; Bohé, L.; Crich, D. The Experimental Evidence in Support of Glycosylation Mechanisms at the S_N1 – S_N2 Interface. *Chem. Rev.* **2018**, *118*, 8242–8284. [[CrossRef](#)]
35. Crich, D. En Route to the Transformation of Glycoscience: A Chemist's Perspective on Internal and External Crossroads in Glycochemistry. *J. Am. Chem. Soc.* **2021**, *143*, 17–34. [[CrossRef](#)]
36. Andreana, P.R.; Crich, D. Guidelines for *O*-Glycoside Formation from First Principles. *ACS Cent. Sci.* **2021**, *7*, 1454–1462. [[CrossRef](#)]
37. Tanaka, K.; Mori, Y.; Fukase, K. Practical Synthesis of a Man β (1-4)GlcNTroc Fragment via Microfluidic β -Mannosylation. *J. Carbohydr. Chem.* **2009**, *28*, 1–11. [[CrossRef](#)]
38. Tanaka, K.; Fukase, K. Acid-mediated Reactions under Microfluidic Conditions: A New Strategy for Practical Synthesis of Biofunctional Natural Products. *Beilstein J. Org. Chem.* **2009**, *5*, 40. [[CrossRef](#)]
39. Tanaka, K.; Fukase, K. Renaissance of Traditional Organic Reactions under Microfluidic Conditions: A New Paradigm for Natural Products Synthesis. *Org. Process Res. Dev.* **2009**, *13*, 983–990. [[CrossRef](#)]
40. Tanaka, K.; Miyagawa, T.; Fukase, K. Chemical *N*-Glycosylation by Asparagine under Integrated Microfluidic/Batch Conditions. *Synlett* **2009**, 1571–1574. [[CrossRef](#)]
41. Uchinashi, Y.; Nagasaki, M.; Zhou, J.; Tanaka, K.; Fukase, K. Reinvestigation of the C5-Acetamide Sialic Acid Donor for α -Selective Sialylation: Practical Procedure under Microfluidic Conditions. *Org. Biomol. Chem.* **2011**, *9*, 7243–7248. [[CrossRef](#)]
42. Uchinashi, Y.; Tanaka, K.; Manabe, Y.; Fujimoto, Y.; Fukase, K. Practical and Efficient Method for α -Sialylation with an Azide Sialyl Donor Using a Microreactor. *J. Carbohydr. Chem.* **2014**, *33*, 55–67. [[CrossRef](#)]
43. Nagasaki, M.; Manabe, Y.; Minamoto, N.; Tanaka, K.; Silipo, A.; Molinaro, A.; Fukase, K. Chemical Synthesis of a Complex-Type *N*-Glycan Containing a Core Fucose. *J. Org. Chem.* **2016**, *81*, 10600–10616. [[CrossRef](#)] [[PubMed](#)]
44. Fukase, K.; Tanaka, K.; Fujimoto, Y.; Shimoyama, A.; Manabe, Y. Sugar Synthesis by Microfluidic Techniques. In *Glycochemical Synthesis*; Hung, S.-C., Zulueta, M.M.L., Eds.; Wiley Online Books; Wiley: Hoboken, NJ, USA, 2016; pp. 205–219. [[CrossRef](#)]
45. Myachin, I.V.; Orlova, A.V.; Kononov, L.O. Glycosylation in Flow: Effect of the Flow Rate and Type of the Mixer. *Russ. Chem. Bull.* **2019**, *68*, 2126–2129. [[CrossRef](#)]
46. Boons, G.J.; Demchenko, A.V. Recent Advances in *O*-Sialylation. *Chem. Rev.* **2000**, *100*, 4539–4566. [[CrossRef](#)] [[PubMed](#)]
47. De Meo, C.; Jones, B.T. Chapter Two—Chemical Synthesis of Glycosides of *N*-Acetylneuraminic Acid. *Adv. Carbohydr. Chem. Biochem.* **2018**, *75*, 215–316. [[CrossRef](#)]
48. De Meo, C.; Goeckner, N. 2.07—Synthesis of Glycosides of Sialic Acid. In *Comprehensive Glycoscience*, 2nd ed.; Barchi, J.J., Vidal, S., Eds.; Elsevier: Amsterdam, The Netherlands, 2021; Volume 2, pp. 228–266. [[CrossRef](#)]
49. Kononov, L.O. Chemical Reactivity and Solution Structure: On the Way to a Paradigm Shift? *RSC Adv.* **2015**, *5*, 46718–46734. [[CrossRef](#)]
50. Ahmed-Omer, B.; Barrow, D.A.; Wirth, T. Heck Reactions using Segmented Flow Conditions. *Tetrahedron Lett.* **2009**, *50*, 3352–3355. [[CrossRef](#)]
51. Kononov, L.O.; Malysheva, N.N.; Kononova, E.G.; Orlova, A.V. Intermolecular Hydrogen-bonding Pattern of a Glycosyl Donor: The Key to Understanding the Outcome of Sialylation. *Eur. J. Org. Chem.* **2008**, *2008*, 3251–3255. [[CrossRef](#)]
52. Kononov, L.O.; Malysheva, N.N.; Orlova, A.V.; Zinin, A.I.; Laptinskaya, T.V.; Kononova, E.G.; Kolotyrykina, N.G. Concentration Dependence of Glycosylation Outcome: A Clue to Reproducibility and Understanding the Reasons Behind. *Eur. J. Org. Chem.* **2012**, *2012*, 1926–1934. [[CrossRef](#)]
53. Kononov, L.O. Modulation of Stereoselectivity of Glycosylation: A Supramer Approach. In *Advances in Chemistry Research*; Taylor, J.C., Ed.; Nova Science Publishers, Inc.: Hauppauge, NY, USA, 2013; Volume 18, pp. 143–178.
54. Ahiadorme, D.A.; Podvalnyy, N.M.; Orlova, A.V.; Chizhov, A.O.; Kononov, L.O. Glycosylation of Dibutyl Phosphate Anion with Arabinofuranosyl Bromide: Unusual Influence of Concentration of the Reagents on the Ratio of Anomeric Glycosyl Phosphates Formed. *Russ. Chem. Bull.* **2016**, *65*, 2776–2778. [[CrossRef](#)]

55. Kononov, L.O.; Fedina, K.G.; Orlova, A.V.; Kondakov, N.N.; Abronina, P.I.; Podvalnyy, N.M.; Chizhov, A.O. Bimodal Concentration-dependent Reactivity Pattern of a Glycosyl Donor: Is the Solution Structure Involved? *Carbohydr. Res.* **2017**, *437*, 28–35. [[CrossRef](#)] [[PubMed](#)]
56. Nagornaya, M.O.; Orlova, A.V.; Stepanova, E.V.; Zinin, A.I.; Laptinskaya, T.V.; Kononov, L.O. The Use of the Novel Glycosyl Acceptor and Supramer Analysis in the Synthesis of Sialyl- α (2–3)-Galactose Building Block. *Carbohydr. Res.* **2018**, *470*, 27–35. [[CrossRef](#)]
57. Orlova, A.V.; Laptinskaya, T.V.; Malysheva, N.N.; Kononov, L.O. Light Scattering in Non-Aqueous Solutions of Low-Molecular-Mass Compounds: Application for Supramer Analysis of Reaction Solutions. *J. Solut. Chem.* **2020**, *49*, 629–644. [[CrossRef](#)]
58. Orlova, A.V.; Ahiadorme, D.A.; Laptinskaya, T.V.; Kononov, L.O. Supramer Analysis of 2,3,5-tri-*O*-Benzoyl- α -D-Arabinofuranosyl Bromide Solutions in Different Solvents: Supramolecular Aggregation of Solute Molecules in 1,2-Dichloroethane Mediated by Halogen Bonds. *Russ. Chem. Bull.* **2021**, *70*, 2214–2219. [[CrossRef](#)]
59. Baker, A.; Graz, M.; Saunders, R.; Evans, G.J.S.; Kaul, S.; Wirth, T. Flow Synthesis of Symmetrical Di- and Trisulfides Using Phase-Transfer Catalysis. *J. Flow Chem.* **2013**, *3*, 118–121. [[CrossRef](#)]
60. Hisamoto, H.; Saito, T.; Tokeshi, M.; Hibara, A.; Kitamori, T. Fast And High Conversion Phase-Transfer Synthesis Exploiting the Liquid–Liquid Interface Formed in a Microchannel Chip. *Chem. Commun.* **2001**, *1*, 2662–2663. [[CrossRef](#)]
61. Ueno, M.; Hisamoto, H.; Kitamori, T.; Kobayashi, S. Phase-Transfer Alkylation Reactions using Microreactors. *Chem. Commun.* **2003**, *3*, 936–937. [[CrossRef](#)]
62. Orlova, A.V.; Andrade, R.R.; da Silva, C.O.; Zinin, A.I.; Kononov, L.O. Polarimetry as a Tool for the Study of Solutions of Chiral Solutes. *ChemPhysChem* **2014**, *15*, 195–207. [[CrossRef](#)] [[PubMed](#)]
63. Kononov, L.O.; Magnusson, G. Synthesis of Methyl and Allyl α -Glycosides of *N*-Acetylneuraminic Acid in the Absence of Added Promoter. *Acta Chem. Scand.* **1998**, *52*, 141–144. [[CrossRef](#)]
64. Kulikova, N.Y.; Shpirt, A.M.; Chinarev, A.; Kononov, L.O. Synthesis of *O*-Acetylated *N*-Acetylneuraminic Acid Glycol. In *Carbohydrate Chemistry: Proven Synthetic Methods*; Kovac, P., Ed.; CRC Press-Taylor & Francis Group: Boca Raton, FL, USA, 2012; Volume 1, pp. 245–250. [[CrossRef](#)]
65. Reynolds, O. XXIX. An Experimental Investigation of the Circumstances which Determine whether the Motion of Water Shall be Direct or Sinuous, and of the Law of Resistance in Parallel Channels. *Philos. Trans. R. Soc. Lond.* **1883**, *174*, 935–982. [[CrossRef](#)]
66. Jahnisch, K.; Hessel, V.; Löwe, H.; Baerns, M. Chemistry in Microstructured Reactors. *Angew. Chem. Int. Ed.* **2004**, *43*, 406. [[CrossRef](#)] [[PubMed](#)]
67. Elvira, K.S.; I Solvas, X.C.; Wootton, R.C.R.; Demello, A.J. The Past, Present and Potential for Microfluidic Reactor Technology in Chemical Synthesis. *Nat. Chem.* **2013**, *5*, 905–915. [[CrossRef](#)]
68. Wang, Q.; Steinbock, O. Materials Synthesis and Catalysis in Microfluidic Devices: Prebiotic Chemistry in Mineral Membranes. *ChemCatChem* **2020**, *12*, 63–74. [[CrossRef](#)]
69. Fang, W.-F.; Yang, J.-T. A Novel Microreactor with 3D Rotating Flow to Boost Fluid Reaction and Mixing of Viscous Fluids. *Sens. Actuators B* **2009**, *140*, 629–642. [[CrossRef](#)]
70. Chen, Y.-T.; Fang, W.-F.; Liu, Y.-C.; Yang, J.-T. Analysis of Chaos and FRET Reaction in Split-and-Recombine Microreactors. *Microfluid. Nanofluid.* **2011**, *11*, 339–352. [[CrossRef](#)]
71. Chen, Y.T.; Chen, K.H.; Fang, W.F.; Tsai, S.H.; Fang, J.M.; Yang, J.T. Flash Synthesis of Carbohydrate Derivatives in Chaotic Microreactors. *Chem. Eng. J.* **2011**, *174*, 421–424. [[CrossRef](#)]
72. deMello, A.J. Control and Detection of Chemical Reactions in Microfluidic Systems. *Nature* **2006**, *442*, 394–402. [[CrossRef](#)]
73. Bothe, D.; Stemich, C.; Warnecke, H.-J. Fluid Mixing in a T-Shaped Micro-Mixer. *Chem. Eng. Sci.* **2006**, *61*, 2950–2958. [[CrossRef](#)]
74. Kockmann, N.; Kiefer, T.; Engler, M.; Woias, P. Convective Mixing and Chemical Reactions in Microchannels with High Flow Rates. *Sens. Actuators B* **2006**, *117*, 495–508. [[CrossRef](#)]
75. Rahimi, M.; Azimi, N.; Parsamogadam, M.A.; Rahimi, A.; Masahy, M.M. Mixing Performance of T, Y, and Oriented Y-Micromixers with Spatially Arranged Outlet Channel: Evaluation with Villermaux/Dushman Test Reaction. *Microsyst. Technol.* **2017**, *23*, 3117–3130. [[CrossRef](#)]
76. Zhang, H.; Kopfmüller, T.; Achermann, R.; Zhang, J.; Teixeira, A.; Shen, Y.; Jensen, K.F. Accessing Multidimensional Mixing via 3D Printing and Showerhead Micromixer Design. *AIChE J.* **2020**, *66*, e16873. [[CrossRef](#)]
77. Kononov, L.O.; Tsvetkov, D.E.; Orlova, A.V. Conceivably the First Example of a Phase Transition in Aqueous Solutions Of Oligosaccharide Glycosides. Evidence from Variable-Temperature ^1H NMR and Optical Rotation Measurements for a Solution of Allyl Lactoside. *Russ. Chem. Bull.* **2002**, *51*, 1337–1338. [[CrossRef](#)]
78. Orlova, A.V.; Zinin, A.I.; Kononov, L.O. Mutarotation in Aqueous Solutions of D-Levogluconan: A Supramer Approach. *Russ. Chem. Bull.* **2014**, *63*, 295–297. [[CrossRef](#)]
79. Orlova, A.V.; Kononov, L.O. Polarimetry as a Method for Studying the Structure of Aqueous Carbohydrate Solutions: Correlation with Other Methods. *RENSIT* **2020**, *12*, 95–106. [[CrossRef](#)]
80. Orlova, A.V.; Laptinskaya, T.V.; Bovin, N.V.; Kononov, L.O. Differences in Reactivity of *N*-Acetyl- and *N,N*-Diacetylsialyl Chlorides, Caused by Their Different Supramolecular Organization in Solutions. *Russ. Chem. Bull.* **2017**, *66*, 2173–2179. [[CrossRef](#)]
81. Sedlák, M. Large-scale Supramolecular Structure in Solutions of Low Molar Mass Compounds and Mixtures of Liquids: I. Light Scattering Characterization. *J. Phys. Chem. B* **2006**, *110*, 4329–4338. [[CrossRef](#)]

82. Sedláč, M. Large-scale Supramolecular Structure in Solutions of Low Molar Mass Compounds and Mixtures of liquids: II. Kinetics of the Formation and Long-time Stability. *J. Phys. Chem. B* **2006**, *110*, 4339–4345. [[CrossRef](#)]
83. Sedláč, M. Large-scale Supramolecular Structure in Solutions of Low Molar Mass Compounds and Mixtures of Liquids. III. Correlation with Molecular Properties and Interactions. *J. Phys. Chem. B* **2006**, *110*, 13976–13984. [[CrossRef](#)] [[PubMed](#)]
84. Sedláč, M.; Rak, D. Large-Scale Inhomogeneities in Solutions of Low Molar Mass Compounds and Mixtures of Liquids: Supramolecular Structures or Nanobubbles? *J. Phys. Chem. B* **2013**, *117*, 2495–2504. [[CrossRef](#)] [[PubMed](#)]
85. Sedláč, M.; Rak, D. On the Origin of Mesoscale Structures in Aqueous Solutions of Tertiary Butyl Alcohol: The Mystery Resolved. *J. Phys. Chem. B* **2014**, *118*, 2726–2737. [[CrossRef](#)] [[PubMed](#)]
86. Rak, D.; Ovadová, M.; Sedláč, M. (Non)existence of Bulk Nanobubbles: The Role of Ultrasonic Cavitation and Organic Solutes in Water. *J. Phys. Chem. Lett.* **2019**, *10*, 4215–4221. [[CrossRef](#)] [[PubMed](#)]
87. Rak, D.; Sedláč, M. On the Mesoscale Solubility in Liquid Solutions and Mixtures. *J. Phys. Chem. B* **2019**, *123*, 1365–1374. [[CrossRef](#)]
88. Rak, D.; Sedláč, M. Solvophobicity-Driven Mesoscale Structures: Stabilizer-Free Nanodispersions. *Langmuir* **2023**, in press. [[CrossRef](#)]
89. Subramanian, D.; Anisimov, M.A. Phase Behavior and Mesoscale Solubilization in Aqueous Solutions of Hydrotropes. *Fluid Phase Equilib.* **2014**, *362*, 170–176. [[CrossRef](#)]
90. Zemb, T.; Kunz, W. Weak Aggregation: State of the Art, Expectations and Open Questions. *Curr. Opin. Colloid Interface Sci.* **2016**, *22*, 113–119. [[CrossRef](#)]
91. Mostafa, S.; Behafarid, F.; Croy, J.R.; Ono, L.K.; Li, L.; Yang, J.C.; Frenkel, A.I.; Cuenya, B.R. Shape-dependent Catalytic Properties of Pt Nanoparticles. *J. Am. Chem. Soc.* **2010**, *132*, 15714–15719. [[CrossRef](#)]
92. Roldan Cuenya, B.; Behafarid, F. Nanocatalysis: Size- and Shape-Dependent Chemisorption and Catalytic Reactivity. *Surf. Sci. Rep.* **2015**, *70*, 135–187. [[CrossRef](#)]
93. Buchecker, T.; Krickl, S.; Winkler, R.; Grillo, I.; Bauduin, P.; Touraud, D.; Pfitzner, A.; Kunz, W. The Impact of the Structuring of Hydrotropes in Water on the Mesoscale Solubilisation of a Third Hydrophobic Component. *Phys. Chem. Chem. Phys.* **2017**, *19*, 1806–1816. [[CrossRef](#)] [[PubMed](#)]
94. Krickl, S.; Touraud, D.; Bauduin, P.; Zinn, T.; Kunz, W. Enzyme Activity of Horseradish Peroxidase in Surfactant-Free Microemulsions. *J. Colloid Interface Sci.* **2018**, *516*, 466–475. [[CrossRef](#)]
95. Hahn, M.; Krickl, S.; Buchecker, T.; Jost, G.; Touraud, D.; Bauduin, P.; Pfitzner, A.; Klamt, A.; Kunz, W. Ab Initio Prediction of Structuring/Mesoscale Inhomogeneities in Surfactant-Free Microemulsions And Hydrogen-Bonding-Free Microemulsions. *Phys. Chem. Chem. Phys.* **2019**, *21*, 8054–8066. [[CrossRef](#)] [[PubMed](#)]
96. Svard, M.; Renuka Devi, K.; Khamar, D.; Mealey, D.; Cheuk, D.; Zeglinski, J.; Rasmuson, A.C. Solute Clustering in Undersaturated Solutions—Systematic Dependence on Time, Temperature and Concentration. *Phys. Chem. Chem. Phys.* **2018**, *20*, 15550–15559. [[CrossRef](#)] [[PubMed](#)]
97. Ding, F.; Ishiwata, A.; Ito, Y. Recent Advances of the Stereoselective Bimodal Glycosylations for the Synthesis of Various Glucans. In *Studies in Natural Products Chemistry*; Elsevier B.V.: Amsterdam, The Netherlands, 2022; Volume 74, pp. 1–40. [[CrossRef](#)]
98. Ishiwata, A.; Tanaka, K.; Ao, J.; Ding, F.; Ito, Y. Recent Advances in Stereoselective 1,2-*cis*-O-Glycosylations. *Front. Chem.* **2022**, *10*, 972429. [[CrossRef](#)] [[PubMed](#)]
99. Zinin, A.I.; Stepanova, E.V.; Jost, U.; Kondakov, N.N.; Shpirt, A.M.; Chizhov, A.O.; Torgov, V.I.; Kononov, L.O. An Efficient Multigram-Scale Synthesis of 4-(*ω*-Chloroalkoxy)phenols. *Russ. Chem. Bull.* **2017**, *66*, 304–312. [[CrossRef](#)]
100. Kulikova, N.Y.; Shpirt, A.M.; Kononov, L.O. A Facile Synthesis of *N*-Acetylneuraminic Acid Glycal. *Synthesis* **2006**, 4113–4114. [[CrossRef](#)]
101. Armarego, W.L.F. *Purification of Laboratory Chemicals*, 8th ed.; Butterworth-Heinemann: Oxford, UK, 2017. [[CrossRef](#)]

Disclaimer/Publisher's Note: The statements, opinions and data contained in all publications are solely those of the individual author(s) and contributor(s) and not of MDPI and/or the editor(s). MDPI and/or the editor(s) disclaim responsibility for any injury to people or property resulting from any ideas, methods, instructions or products referred to in the content.